Free Electron Laser Pumped by a Powerful Traveling Electromagnetic Wave

R. ALAN KEHS, SENIOR MEMBER, IEEE, YUVAL CARMEL, MEMBER, IEEE,
VICTOR L. GRANATSTEIN, SENIOR MEMBER, IEEE, AND WILLIAM W. DESTLER, MEMBER, IEEE

Abstract—**A three-wave free-electron laser (FEL) was operated with a powerful 8.4-GHz electromagnetic "pump" wave replacing the usual magnetostatic wiggler. The presence of a uniform axial magnetic field B_0 produced cyclotron-harmonic "idler" waves. Peaks in the emission spectrum corresponding to cyclotron harmonics were observed covering a frequency range from 16.5 to 130 GHz. The frequency spectrum of this novel FEL mechanism was tuned continuously by the variation of B_0.**

I. Introduction

IN RECENT years there has been strong interest in free-electron lasers (FEL's) for the production of high-power, coherent, tunable electromagnetic radiation. Both two-wave FEL's [1]–[4] and three-wave FEL's [5]–[7] have been demonstrated and have exhibited great potential for extending the available range of wavelength and power levels of coherent sources while maintaining high operating efficiencies. Three-wave FEL's consist of an idler wave on the electron beam, a pump wave, and a radiation wave. Typically, the pump wave is created via a static periodic magnet (wiggler). However, any field that induces a transverse electron oscillation would, in principle, function as a pump field. For example, a static periodic electric field [8] or an electromagnetic field [9] could be used.

In experiments where a solenoidal guide magnetic field is present in addition to the wiggler field, either beam space-charge waves or beam cyclotron waves can act as idlers in a three-wave FEL. The case of an FEL with a space-charge wave idler was carefully studied in the experiments of Fajans *et al.* [10]. The effect of electron-cyclotron motion on FEL operation has been studied both theoretically [11] and in experiments [12]–[14]. The three-wave FEL was a magnetostatic wiggler and fundamental cyclotron-frequency idler was studied experimentally [13], [14], and that work is closely related to the present study.

Recently, powerful radiation at millimeter wavelengths [15], [16] was observed in relativistic backward-wave oscillator experiments in our laboratory, which was designed to generate high-power microwaves at a wavelength of several centimeters and peak power levels of $\simeq 100$ MW [17], [18]. In the present work we present detailed measurements of the spectrum of the millimeter-wave radiation which is observed in very high-power backward-wave oscillators and use the features of the observed spectrum to deduce the radiation mechanism. We found the unexpected result that the millimeter-wave spectrum is composed of an array of regularly spaced peaks. The frequencies of the peaks and their variation with the strength of the axial guide magnetic field indicate that the spectrum is due to a three-wave FEL interaction with cyclotron-harmonic beam waves acting as "idlers," and with the backward-wave oscillator radiation at a frequency of 8.4 GHz acting as the pump wave [19], [20].

This paper is organized as follows: Section II presents a brief review of the classical free electron laser (magnetostatic wiggler) and the electromagnetically pumped free electron laser. In Section III the experimental setup is described. Experimental results, the basic theory of the interaction, and a discussion are presented in Section IV. Portions of this work have been previously reported [19].

II. Review of Classical (Magnetostatic) and Electromagnetically Pumped Free Electron Laser

The theory of the classical (magnetostatically pumped) FEL has been extensively developed [21], [22] and will not be discussed in detail. Although the full theory of electromagnetically pumped free electron lasers is less complete [23], [24] and is also beyond the scope of this paper, a brief physical picture will be presented in conjunction with those portions of the theory needed to predict the complex output spectrum. The electromagnetically pumped FEL is attractive because it enables significant increases in the radiation frequency for the same beam parameters (as compared to the magnetostatic wiggler-driven FEL) and continuous tunability by changing the electromagnetic pump frequency.

There are basically two physical regimes for FEL's: In the collective regime, where the density of the beam is high, the process involves a beam idler wave (such as a slow space-charge or a cyclotron wave), the radiation wave, and the wiggler (magnetostatic and electromagnetic). In this three-wave interaction regime the intense

Manuscript received October 26, 1989; revised January 5, 1990. This work was partially supported by the Harry Diamond Laboratories and the Office of Naval Research.

R. S. Kehs is with the Harry Diamond Laboratories, 2800 Powder Mill Road, Adelphi, MD 20783.

Y. Carmel, V. L. Granatstein, and W. W. Destler are with the Laboratory for Plasma Research, University of Maryland, College Park, MD 20742.

IEEE Log Number 9035365.

electron beams are often moderately relativistic (0.5–2 MeV), as is the case for the work reported here. In the low density ("Compton") regime, the interaction is between the individual electrons, the radiation field, and the undulator. This is a two-wave particle-interaction regime and is characterized by a highly relativistic electron beam (10–1000 MeV).

The most basic free electron laser radiation mechanism is a two-wave interaction in which a transverse, periodicmagnetic field induces oscillations on an intense, energetic electron beam. Using the configuration shown in Fig. 1, an electron beam is injected along the $\hat{z}$ so that it will pass through the spatially varying magnetic field generated by the permanent bar magnets labelled N and S. At the point of interaction the electrons have random phase and radiate incoherently. However, a ponderomotive force is produced by the action of the induced $v_\perp$ (often called the quiver velocity or wiggler velocity) and the radiation (or scattered) wave. Thus from the Lorentz force law,

$$F_{\text{pond}} = -|e| v_\perp \times \boldsymbol{B}_r \tag{1}$$

where $|e|$ is the electronic charge, $v_\perp$ is the wiggler velocity, and $\boldsymbol{B}_r$ is the magnetic component of the scattered electromagnetic wave. This $\hat{z}$-directed force acts to push the electrons into axial bunches. The pondermotive force causes some electrons to be accelerated and others to be decelerated. If the axial velocity of the beam v_{z0} is such that more electrons are decelerated, then the average energy of the electrons decreases and the radiation field is enhanced. Clearly, this process will only proceed when the oscillating electrons are properly synchronized with the electromagnetic wave. This synchronism condition leads directly to a relation for the expected frequency spectrum of the ideal magnetostatic FEL model.

Next, we calculate this synchronism condition and the expected radiation frequency for both the magnetrostatic and electromagnetic pumped FEL's, with and without waveguide effects, for both two- and three-wave FEL's. The FEL interaction occurs when the beam particles see the wiggler and radiation to have the same frequency. For a magnetostatically pumped FEL in free space, the wiggler can be described as

$$B = B_w \sin k_w z. \tag{2}$$

The radiation field is given by

$$E = E_r \sin (\omega_r t \pm k_r z) \tag{3}$$

where the $+/-$ indicate backward/forward propagating waves and the beam motion is given by

$$z = v_\parallel t. \tag{4}$$

In the above equations k_w, k_r, ω_r, and $v_\parallel$ are the wiggler wavenumber, radiation wavenumber, angular radiation frequency, and beam velocity, respectively. With $\omega_r = k_r c$, where c is the speed of light, the resonance condition is therefore reached by equating the phases in (2) and (3)

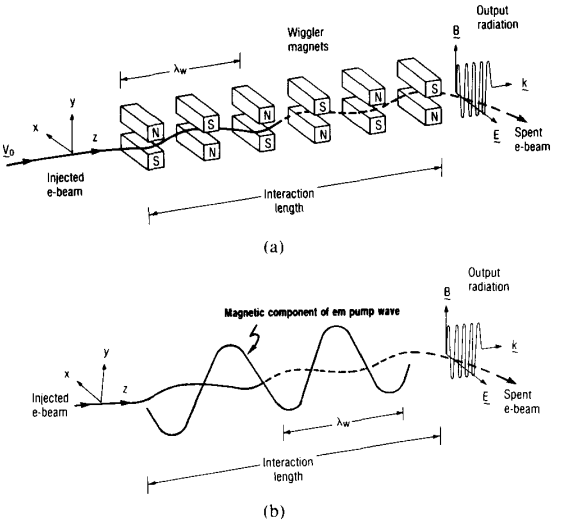

Fig. 1. The basic free electron laser interaction. (a) Magnetostatic pump. (b) Electromagnetic pump.

and using (4) to obtain:

$$\frac{k_r}{k_w} = (1 \mp \beta_\parallel)\beta_\parallel \gamma_\parallel^2 \tag{5}$$

where the $+/-$ signs correspond to frequency down/up conversion, and $\beta_\parallel \equiv v_\parallel / c$. This can also be written as

$$\omega_r = (k_w \pm k_r) v_\parallel. \tag{6}$$

Similarly, for electromagnetically pumped FEL's, the wiggler field can be described by

$$B = B_w \sin (k_w z + \omega_w t) \tag{7}$$

where ω_w is the angular frequency of the pump wave and the radiation field is given by

$$E = E_r \sin (\omega_r t \mp k_r z). \tag{8}$$

By using $\omega_w = k_w v_{\text{ph}}$, where v_{ph} is the phase velocity of the pump wave, the resonance condition for an electromagnetically pumped FEL can now be cast in a form similar to (5):

$$\frac{k_r}{k_{w_{\text{eq}}}} = (1 \mp \beta_\parallel)\beta_\parallel \gamma_\parallel^2 \tag{9}$$

where the equivalent wiggler wave number is now defined as

$$k_{w_{\text{eq}}} = k_w \frac{\beta_{\text{ph}}}{\beta_\parallel}(1 + v_\parallel / v_{\text{ph}}) = \frac{\omega_w}{v_\parallel}\left(1 + \frac{v_\parallel}{v_{\text{ph}}}\right). \tag{10}$$

This resonance condition can also be written in a form similar to (6); namely,

$$\omega_r - \omega_w = (k_{w_{\text{eq}}} \pm k_r) v_\parallel. \tag{11}$$

The preceding analysis is appropriate for low-density electron beams in which single-particle equations can be

used to describe the interactions; i.e., the Compton regime. For higher density electron beams, collective effects become important and beam waves or "idlers" can participate in a more complicated three-wave interaction—the Raman regime. The FEL described in this paper operates in this high beam-density Raman regime.

The basic approaches used to describe the expected output from a two-wave single particle FEL interaction can be expanded to include the effect of the "idler" wave which participates in three-wave FEL interactions.

A high-current electron beam propagating through an axial magnetic field can support several types of "beam idlers" [25]. The most important types (and the only ones that will be considered in this report) are the natural plasma resonances; namely, the negative energy space-charge and cyclotron waves and their harmonics. These waves can interact with the pump wave to efficiently couple energy from the electron beam into "scattered radiation" via a three-wave interaction where the idler acts as a low-frequency "beat" wave.

The effect of idlers on the resonance condition results in an additional shift in the radiation frequency given by (5) and (10). For the case of an electromagnetically pumped FEL, (10) now becomes

$$\omega_r - \omega_w = (k_{w_{eq}} \pm k_r)v_\parallel \pm \omega_{idler} \tag{12}$$

where ω_{idler} is given by

$$\omega_{idler} = \begin{cases} m\omega_b, & \text{for space-charge idlers } (\omega_b = \text{angular plasma frequency of beam}) \\ l\Omega_0, & \text{for cyclotron idlers } (\Omega_0 = \text{angular relativistic electron-cyclotron frequency}). \end{cases}$$

Here m and l are integer harmonic numbers.

The resonance conditions given by (5), (10), and, in particular, (12) can now be extended to include the effects of a finite transverse-interaction region. The amplified FEL wave propagates inside a drift tube which acts like a waveguide. The waveguide modes are characterized by a low-frequency cutoff, and therefore the FEL radiation frequency will be most strongly affected in the vicinity of this cutoff. The frequency and wavenumber in the waveguide must satisfy

$$\omega_r^2 = k_r^2 c^2 + \omega_{co}^2 \tag{13}$$

where ω_{co} represents the mode-dependent cutoff frequency of the waveguide. Radiation growth occurs near frequencies corresponding to the crossing points of the dispersion curves represented by (12) and (13). Solving (12) and (13) simultaneously yields the frequencies of two unstable classes of modes; viz.,

$$\omega_r = \omega_\parallel \gamma_\parallel^2 c K_{eff} \left\{ 1 \pm \beta_\parallel \left[1 - \left(\frac{\omega_{co}}{K_{eff}\gamma_\parallel \beta_\parallel c} \right)^2 \right]^{1/2} \right\}. \tag{14}$$

Here the $+/-$ sign in (14) represents the up- and downshifted interaction branches, and K_{eff} now includes the effects of the idlers.

This expression can be used to calculate the radiation frequency of two- and three-wave FEL's, magnetostatically and electromagnetically pumped, including the effect of the waveguide. The definitions of K_{eff} that correspond to various FEL mechanisms are given in Table I.

An idealized dispersion relation for an electromagnetically pumped FEL with space-charge and cyclotron idlers is shown in Fig. 2. In this figure the up- and downshifted interaction frequencies are marked with circles.

It is important to note that if we consider the various cyclotron-harmonic idlers ($l > 1$) and a fixed value of the applied axial magnetic field is chosen, then a whole spectrum of regularly spaced peaks should be produced by this interaction. Although some of the even harmonics were omitted from Fig. 3 for clarity, all harmonics are present in any spectrum which can be modeled by (14) for the case of cyclotron-harmonic idlers. Fig. 3 corresponds to the experimental parameters that will be described in the following sections.

The line width of an electromagnetically pumped FEL will depend on the natural line width and will also be subject to broadening due to the finite pulse duration and to the finite spectrum of the electromagnetic pump. It is expected that the pump line width will translate into the FEL line width according to

$$\frac{\Delta\omega_r}{\omega_r} = \frac{\Delta\omega_w}{\omega_w}. \tag{15}$$

This point will be further discussed in Section IV.

III. The Experimental Setup

The electromagnetically pumped FEL experiment was designed to use only a single electron beam. The relativistic electron beam initially generated a powerful electromagnetic wave by interaction with a corrugated waveguide structure, and thus exciting a backward propagating mode at 8.4 GHz. This backward wave served as the pump wave for the FEL interaction. The two processes develop simultaneously on the same electron beam, thereby producing coherent millimeter wave radiation as well as powerful centimeter wavelength microwaves.

A schematic of the experimental concept showing the principal wave traffic is shown in Fig. 4. An annular relativistic electron beam (625 kV, 2 kA, 100 ns) is guided by a strong axial magnetic field through a corrugated slow-wave structure. The slow-wave structure allows the electron beam to couple kinetic energy from the beam into an electromagnetic mode of the structure which propagates antiparallel to the electron beam. This backward propagating mode (TM_{01}) provides the pump wave for the FEL interaction. Both the pump and scattered radiation are reflected by the mirror, and both are detected downstream.

The basic experimental configuration is shown in Fig. 5. The electron beam is generated by a field emission

TABLE I
DEFINITION OF K_{eff} FOR VARIOUS FEL MECHANISMS

FEL Mechanism	K_{eff}
Two-wave FEL with Magnetostatic Pump	$\frac{2\pi}{\ell_w}$
Two-wave FEL with Electromagnetic Pump	$\frac{\omega_w}{\beta_\parallel c}\left[1+\frac{\beta_\parallel}{\beta_{ph}}\right]$
Three-wave FEL with Electromagnetic Pump and Cyclotron Harmonic Idler	$\frac{\omega_w}{\beta_\parallel c}\left(1+\frac{\beta_\parallel}{\beta_{ph}}\right)+\frac{\ell\Omega_0}{\beta_\parallel c}$
Cyclotron Harmonic Autoresonance Maser (CHARM)	$\frac{\ell\Omega}{\beta_\parallel c}$
Three-wave FEL with Electromagnetic Pump and Space Charge Harmonic Idler	$\frac{\omega_w}{\beta_\parallel c}\left[1+\frac{\beta_\parallel}{\beta_{ph}}\right]+\frac{m\omega_b}{\beta_\parallel c}$
Three-wave FEL with Magnetostatic Pump and Cyclotron Harmonic Idler	$\frac{2\pi}{\ell_w}+\frac{\ell\Omega_0}{\beta_\parallel c}$
Three-wave FEL with Magnetostatic Pump and Space Charge Harmonic Idler	$\frac{2\pi}{\ell_w}+\frac{m\omega_b}{\beta_\parallel c}$

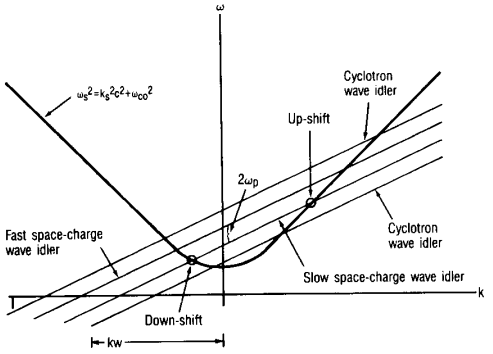

Fig. 2. Idealized dispersion diagram for EM-pumped FEL with space-charge and cyclotron idlers.

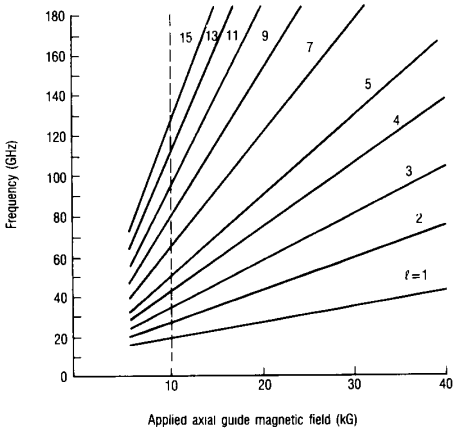

Fig. 3. Plot of interaction frequency versus applied magnetic field for several harmonics of the EM-pumped FEL with cyclotron harmonic idlers.

cathode immersed in an axial magnetic field and driven by a pulse line accelerator [26]. A 1-m long solenoid was used to produce fields up to 23 kG inside the device, which operated at a background pressure of $\sim 10^{-6}$ torr.

In addition to a variety of probes used for measuring the beam parameters, microwave and millimeter wave diagnostics were also used. The microwave diagnostic system used to measure the frequency spectrum from 7–18 GHz is shown in Fig. 6. An array of band-pass and low-pass filters as well as dispersive lines and heterodyne mixers were used to measure the power and frequency in this band [27]. Measurements of the millimeter spectrum (FEL radiation) were made from 50 to 130 GHz using a grating spectrometer [28] having a resolving power $\Delta f/f = 2\%$ (see Fig. 7).

A BWO was chosen as the electromagnetic pump generator because of its high-power handling capabilities. To

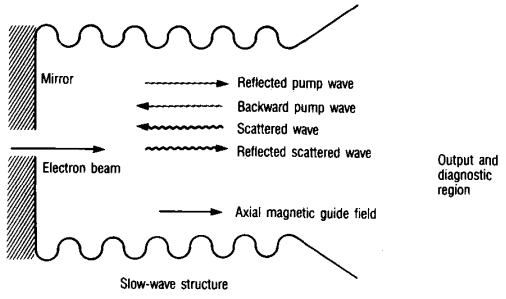

Fig. 4. Principal wave traffic in an FEL pumped by a powerful traveling electromagnetic wave.

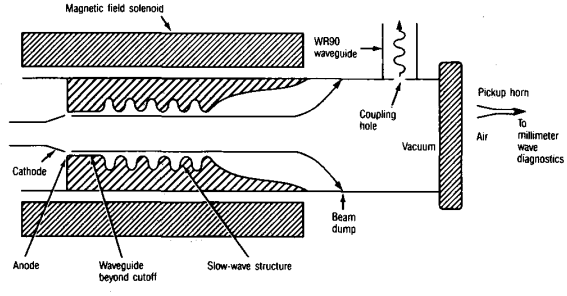

Fig. 5. The basic experimental configuration used for pumping an FEL with a powerful traveling electromagnetic wave (not to scale).

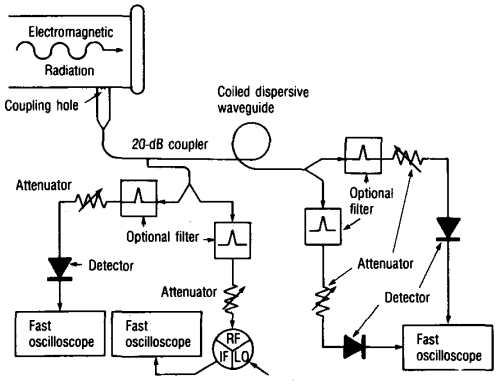

Fig. 6. Schematic drawing of the high-power microwave diagnostic system (7–20 GHz).

equal the strength of a 300-G magnetostatic pump, the power of an electromagnetic wave in a 3-cm diam wave guide should be ~50 MW. The BWO mechanism can easily generate these power levels and more in the fundamental TM_{01} mode [17], [18]. Since the beam is axially symmetric and directed in the z direction, one anticipates a strong coupling of the beam energy to the TM_{01} mode of the corrugated structure. The dispersion relation for an infinitely long structure with a periodicity of 1.67 cm and corrugation amplitude of ±27% (the experimental value) is given in Fig. 8 [29]. Also superimposed in the same figure is the beam's space-charge wave-dispersion relation given by

$$\omega = v_{\parallel}(k \mp 2\pi n/L) \qquad (16)$$

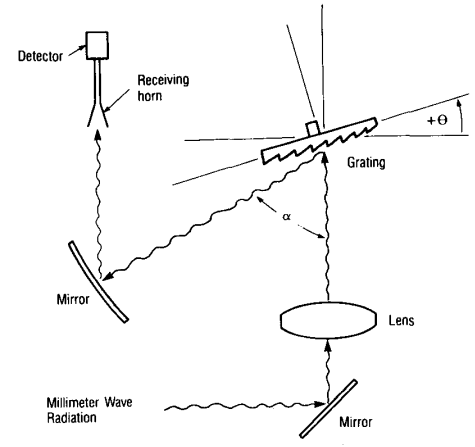

Fig. 7. Schematic drawing of the millimeter wave grating spectrometer used from 50 to 130 GHz.

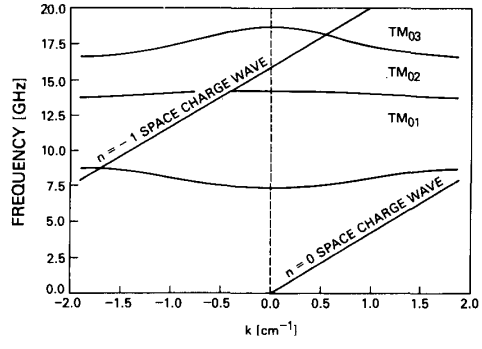

Fig. 8. The empty corrugated waveguide dispersion diagram for symmetric TM modes, with superimposed ideal space-change beam waves.

where n is the spatial harmonic number and L is the period of the ripples on the slow wave structure.

Finally, the BWO operated at a beam current of 2.3 kA, which is about three times the start oscillation current [30].

IV. Results and Discussion

The measured spectrum of the millimeter wave radiation exhibits a distinct line structure of regularly spaced peaks, as shown in Fig. 9(a). In Fig. 9(b) the spectra corresponding to two different values of magnetic field are plotted. It can be clearly seen that the entire frequency spectrum is shifted when the magnitude of the guide field is changed. The frequency spectrum was tuned continuously by varying the guiding magnetic field. Although not shown in this section, spectra were also measured for several other values of the magnetic field, including 11.4, 19.4, and 20.3 kG. Regularly spaced peaks were always present. The frequencies of the peaks and their variation with the strength of the axial magnetic guide field indicate that the spectrum is due to a three-wave FEL interaction in which cycloton harmonic beam waves act as "idlers." There is an excellent match between the experimental data

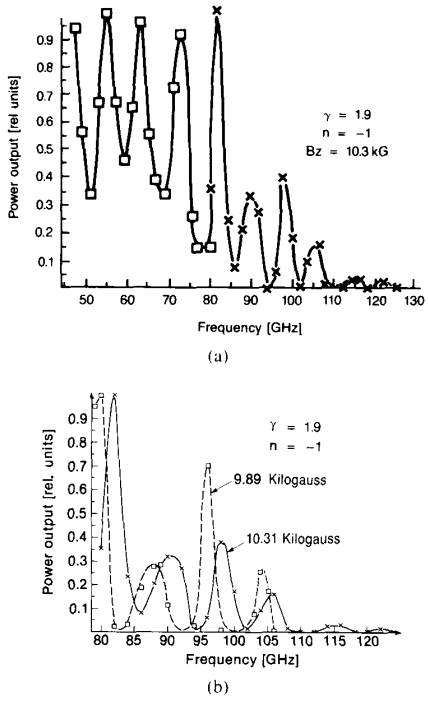

Fig. 9. The measured frequency spectrum (a) from 50 to 125 GHz for an applied field of 10.3 kG; and (b) from 80 to 125 GHz for applied fields of 9.89 and 10.3 kG.

and the prediction of the model represented by (13), as will be discussed shortly. Also, a detailed examination of low-frequency, low-harmonic number data will be used to demonstrate that the emission spectrum is due to an FEL interaction, and not to a CHARM interaction. This is important because of the close similarity between the FEL and CHARM spectra—especially at the higher frequencies.

An electromagnetic pump wave incident on the electrons can result in the development of body "idler" cyclotron harmonic waves and a backscattered electromagnetic wave. This situation can be clearly visualized using the Stokes diagram in the laboratory frame, as shown in Fig. 10. The interaction can be based on one of many cyclotron harmonic numbers, where only one of them (second harmonic) is shown in the figure for clarity. Different harmonic numbers will introduce changes in the radiation frequency (ω_r), and a spectrum having regularly space peaks is expected.

The idealized dispersion relation for the electromagnetically pumped FEL with cyclotron-harmonic idlers is shown in Fig. 11. There are two allowed interaction frequencies for each harmonic number—an "upshifted" and a "downshifted" frequency. Actually, both interaction frequencies are generally higher than the pump frequency, but convention refers to the higher as upshifted and the lower as downshifted. In Fig. 11 the lower downshifted interaction frequencies are marked with circles.

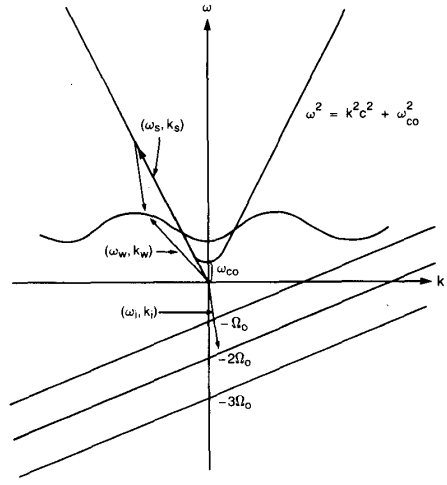

Fig. 10. Stokes diagram of the three-wave FEL interaction with the backward propagating pump wave, the slow cyclotron harmonic wave idler, and scattered radiation along the "downshifted" branch. (Laboratory reference frame.)

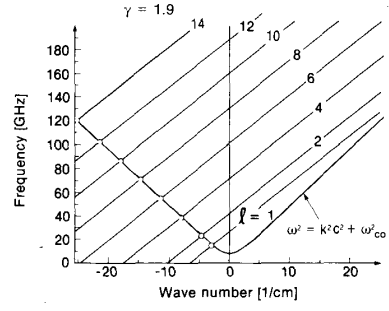

Fig. 11. Simplified dispersion relations of the waveguide mode and the cyclotron-harmonic mode downshifted by the electromagnetic wiggler.

As was shown in Section II, the radiation frequency for an electromagnetically pumped FEL with a cyclotron harmonic is given by (13), and K_{eff} (defined in Table I) is

$$K_{\text{eff}} = \frac{\omega_w}{\beta_\parallel c}\left[1 + \frac{\beta_\parallel}{\beta_{\text{ph}}}\right] + \frac{l\Omega_0}{\beta_\parallel c}. \tag{17}$$

For the experimental data presented in Fig. 9, the minimum observed frequency was 50 GHz, and the waveguide effects can be ignored ($\omega_{co} \to 0$). Equation (14) can then be reduced and cast in terms of frequencies to become:

$$f_r = \gamma_\parallel^2\left[f_w\left(1 + \frac{\beta_\parallel}{\beta_{\text{ph}}}\right) + lf_{ce}\right](1 \pm \beta_\parallel) \tag{18}$$

where f_r and f_w are the frequencies of the scattered and pump waves, and f_{ce} is the relativistic electron-cyclotron frequency.

The parameters (corresponding to the experimental conditions) used for the calculations are shown in Table II. Both the theoretical (equation (18)) and the experimental results are superimposed in Fig. 12(a) and (b).

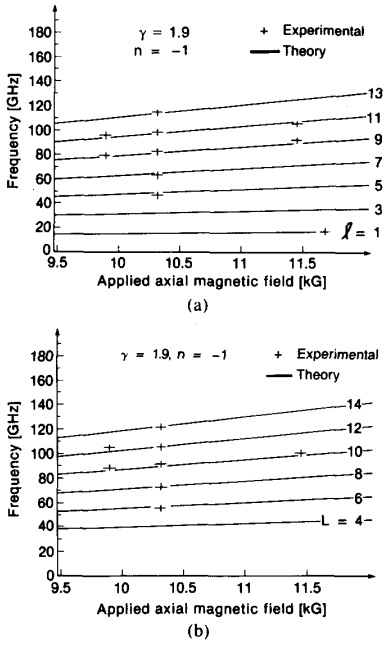

Fig. 12. Dependence of the frequency peaks on magnetic field for odd harmonic numbers from 1 through 15: (a) and even harmonic numbers from 4 through 14; and (b) with crosses marking the positions of the measured peaks.

TABLE II
THE PARAMETERS (CORRESPONDING TO THE EXPERIMENTAL CONDITIONS) USED FOR THE CALCULATIONS PRESENTED IN FIG. 12(a) AND (b)

f_w	8.4 GHz
$\gamma_\parallel$	1.9
$\beta_\parallel$	0.85
β_{ph}	1.054
f_{co}	$2.8/\gamma_\parallel$ GHz/kG
ℓ	1 to 14

The two most convincing aspects of the fit between theory and experiment are the peak spacing and magnetic field dependence. Harmonic numbers $l = 1$ and 5 through 14 were identified during the scanning of most of the spectrum between 7 and 130 GHz. Furthermore, the locations of the measured spectral peaks move with the axial magnetic field, which would not be expected in the FEL with the space-charge idler. Adequate microwave diagnostics were not available for the range from 18.6 to 50 GHz where harmonic numbers $l = 2$, 3, and 4 were predicted to appear. Fig. 12 shows the excellent match between the theoretical predictions for the frequency shift and experimental results.

This frequency shift with magnetic guide field is especially important because it not only eliminates several prospective mechanisms for high-frequency microwave production but also eliminates the possibility that the peaks were due to resonances in the diagnostic system.

The experimental results presented so far clearly fit the mechanism of an electromagnetically pumped FEL with cyclotron-harmonic idlers. The measured spectra in the range 50–130 GHz correspond to the downshifted resonance condition when the FEL is pumped by a backward wave. Nevertheless, it must also be shown that other computing mechanisms are inappropriate.

Models based on the excitation of higher order modes in the BWO can easily be dismissed by considering the experimental frequency shift versus magnetic field. The higher order modes are solely a function of the geometry and do not depend on the applied magnetic field strength.

Other radiation mechanisms with somewhat similar spectra are the FEL pumped by a forward pump ($\beta_{ph} \rightarrow -\beta_{ph}$) and the counterwave cyclotron-harmonic autoresonant maser for which we coin the acronym CHARM [31], [32]. The spectra of these mechanisms is significantly different from that of an FEL pumped by the backward wave for low frequencies; i.e., low-harmonic number ($l < 3$). The experimental data for low-harmonic numbers will be used to distinguish between the above mechanisms because of the close similarity of the spectra at high-harmonic numbers.

For example, the forward-wave FEL model predicts interactions at both 10.4 and 17.6 GHz, while the backward-wave model predicts only a single interaction at 17 GHz. Careful study of the frequency range from 7–20 GHz revealed peaks at only 8.4 (pump frequency) and 16.5 GHz. As there was no microwave power detected in the frequency range near 10.4 GHz, we can therefore conclude that the forward-wave model can be excluded.

The counterwave CHARM also has a significantly different spectrum at low-harmonic numbers. Specifically, radiation with that mechanism should be produced at 12.5 and 18.2 GHz (for an applied field of 10 kG), but in an intensive spectral search from 7 to 18.6 GHz microwave radiation was only detected at 8.4 GHz, the frequency of the pump wave, and at 16.5 GHz, the $l = 1$ harmonic of the electromagnetically pumped FEL with cyclotron-harmonic idler.

These differences are clearly seen in Fig. 13 in which the downshifted spectra are plotted for the CHARM and backward pump-wave FEL interaction. The solid lines represent theory and the circled crosses denote experimentally measured peaks. A careful search of the microwave spectrum was able to detect power only at the single frequency marked by the circled cross. The data point clearly corresponds to the expected spectrum of the backward wave pump rather than to the expected spectrum of the CHARM interaction. Thus the CHARM model fails to adequately predict the measured frequency spectrum.

In addition to the poor match between low-frequency predictions and experimental data, measurements of the electron-beam parameters indicated that $\beta_\perp < 0.05 \pm 0.01$, which is insufficient for the production of radiation via a CHARM-type interaction. Finally, when a smooth metallic liner was inserted into the drift tube to eliminate the periodic wall, no electromagnetic radiation at any frequency could be detected. This supports the assertion that the observed microwave spectrum was due to a non-

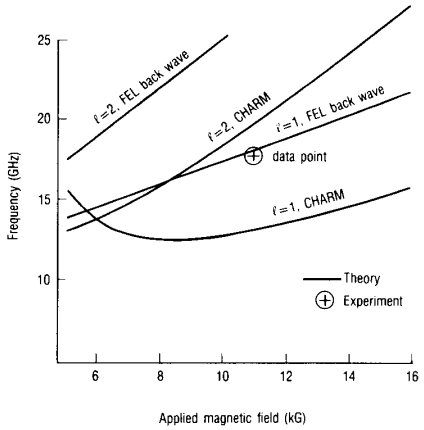

Fig. 13. Low-harmonic interaction frequencies versus the applied magnetic field for downshifted branches of CHARM and EM-pumped FEL with the backward pump wave and cyclotron-harmonic idlers.

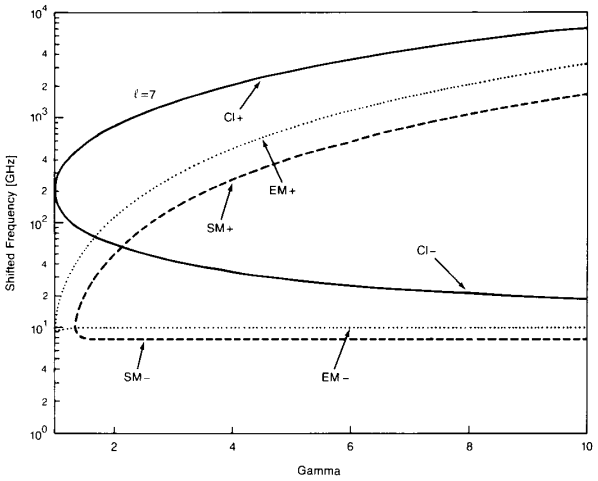

Fig. 14. Frequency scaling versus gamma for several interaction mechanisms where SM, EM, and CI refer to static magnetic, electromagnetic, and electromagnetic with cyclotron-harmonic idler wigglers, respectively, and the +/− refers to the up/downshifted branch.

CHARM-type process. If the radiation leaving the drift chamber (as indicated in Fig. 5) is assumed to be isotropic and the pickup horn is assumed to be in the far-field region, then the power at 16.5 GHz corresponding to $l = 1$ is $\simeq 250$ kW, with decreasing power levels for emission lines corresponding to larger values of l.

Finally, a short discussion of the FEL spectra purity and frequency scaling with energy will be given. As was indicated in Section II, the FEL spectral broadening due to the finite spectral width of the pump wave is expected to follow (14). Since the FWHM relative width of the 8.4-GHz electromagnetic pump is $\sim 2.4\%$, the FEL relative line width is expected to be similar, which is in good agreement with the experimental results ($\sim 2.5\%$) presented in Fig. 9 (although this result is also close to the resolving power of the spectrometer).

An interesting feature of this novel FEL mechanism is its frequency scaling with γ as shown in Fig. 14. Also shown in the figure are the upshifted (+) and downshifted (−) frequency conversion factors for magnetostatically (labeled SM) and electromagnetically (labeled EM) pumped FEL's with space-charge wave idlers. Note that the behavior predicted for a downshifted electromagnetically pumped FEL with a cyclotron-harmonic idler (labeled CI in Fig. 14) is different from the behavior of the other FEL mechanisms. The figure shows the specific scaling law for the harmonic number $l = 7$, but the behavior is typical for all harmonic numbers. The decrease of frequency with increasing γ can easily be understood by referring to (17). There, f_{ce} is the relativistic electron-cyclotron frequency which decreases with increasing γ, and the term lf_{ce} is dominant. Note also that it is possible to tune the frequency of the FEL by varying either the axial magnetic guide field or γ.

V. Conclusion

The work reported here is the first to demonstrate cyclotron-harmonic idlers and is also the first study of the frequency spectrum produced by this class of devices. In fact, the spectrum was carefully resolved from 7–20 and 50–130 GHz. We have demonstrated that electromagnetic pumping in the presence of a uniform axial magnetic field results in a three-wave FEL interaction involving cyclotron-harmonic idler waves. The differences in the spectra predicted by other possible mechanisms were sufficiently distinct that they could be eliminated in favor of the three-wave EM-pumped FEL. This mechanism produced coherent, powerful, millimeter-wave radiation with a relatively modest value of the uniform magnetic field. A continuous tunability over a very wide frequency range is a distinguishing feature of this FEL mechanism. Although the data reported have resulted from the downshifted interaction branch, the same mechanism is also expected to produce much higher frequencies on the upshifted branch for the same electron beam parameters and magnetic field. For example, harmonic $l = 15$ will radiate at 1578 GHz as can be seen from Table III. While the power at 8.4 GHz was about 100 MW, the power in the emission at 16.5 GHz (corresponding to $l = 1$) is estimated at 250 kW, with decreasing power levels for emission lines at larger values of l. Note that the two mechanisms, the BWO and FEL, occur simultaneously, and no effort has been yet made to optimize the FEL interaction.

Also, while the BWO process involves an absolute instability and requires no resonant cavity, the high-frequency FEL process involves a convective instability and can very likely be enhanced by the presence of a resonant cavity of optimized dimensions. Finally, it should be noted that the value of the guide magnetic field for optimizing power in the BWO "pump" may not be the same as required to maximize the FEL output power.

A sketch of a new experimental configuration which we propose to use for characterizing and optimizing the FEL emission is shown in Fig. 15. The region of FEL interaction is separated from the BWO region and will have a

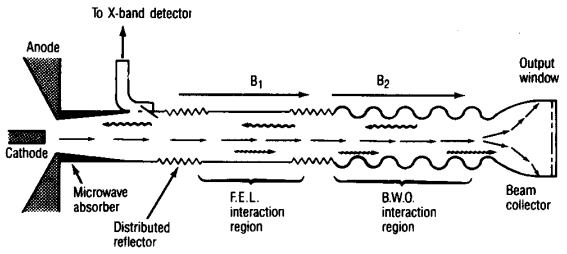

Fig. 15. An improved two-stage BWO/FEL configuration.

TABLE III
THE EXPECTED RADIATION FREQUENCIES FOR EM-PUMPED FEL WITH CYCLOTRON-HARMONIC IDLERS (UP-SHIFTED BRANCH)

ℓ	Frequency (GHz)
1	199.0
2	297.7
3	396.3
4	494.8
5	593.3
6	691.8
7	790.2
8	888.7
9	987.1
10	1085
11	1184
12	1282
13	1381
14	1479
15	1578

separately variable length and guide magnetic field. By separately varying the magnetic field strength in the BWO region, the power in the EM "pump" wave for the FEL process can be controlled and the threshold "pump" power for turning on the FEL can be determined.

Also, in Fig. 15, the distributed feedback is used to define a resonant cavity for the FEL interaction. The distributed feedback could be accomplished by small-scale periodic reflectors (e.g., Bragg reflectors) that will not seriously perturb the 8.4-GHz "pump" wave. The use of distributed reflection to enhance this type of two-stage wave generation has been suggested by Bratman *et al.* [33]. It has been suggested [34], [35] that for a given output wavelength, electron energy requirements could be greatly reduced if a two-stage FEL could be constructed. Such an FEL could operate at a wavelength $\lambda_r \sim l_w/8\gamma^4$. In the present study of a two-stage process, only the second stage is an FEL. We nevertheless expect the insights gained in this study of EM pumping to contribute to a better evaluation of the potential for a two-stage FEL.

ACKNOWLEDGMENT

The authors would like to acknowledge the helpful discussions with G. Bekefi, A. Bromborsky, B. Danley, A. Flitflet, H. Freund, B. Levush, K. Minami, B. Ruth, and J. Wurtele. They also thank D. Presgraves and W. R. Lou for assistance in operating the experiment and Prof. Derek Boyd for his grating spectrometer.

REFERENCES

[1] L. R. Elias, W. M. Fairbank, J. M. J. Madley, H. A. Schwettman, and T. I. Smith, *Phys. Rev. Lett.*, vol. 36, no. 13, pp. 717-720, 1976.
[2] D. A. G. Deacon *et al.*, "First operation of a free-electron laser," *Phys. Rev. Lett.*, vol. 36, no. 16, pp. 892-894, 1977.
[3] B. Girard *et al.*, "Optical frequency multiplication by an optical klystron," *Phys. Rev. Lett.*, vol. 53, no. 25, pp. 2405-2408, 1984.
[4] T. J. Orzechowski *et al.*, "High-efficiency extraction of microwave radiation from a tapered wiggler free-electron laser," *Phys. Rev. Lett.*, vol. 57, no. 17, pp. 2172-2175, 1986.
[5] D. B. McDermott, T. C. Marshall, S. P. Schlesinger, R. K. Parker, and V. L. Granatstein, "High-power free-electron laser based on stimulated Raman scattering," *Phys. Rev. Lett.*, vol. 41, no. 20, pp. 1368-1371, 1978.
[6] R. K. Parker *et al.*, "Axial magnetic-field effects in a collective interaction free-electron laser at millimeter wavelengths," *Phys. Rev. Lett.*, vol. 48, no. 4, pp. 238-242, 1982.
[7] S. H. Gold *et al.*, "High-gain 35-GHz free-electron laser-amplifier experiment," *Phys. Rev. Lett.*, vol. 52, no. 14, pp. 1218-1221, 1984.
[8] G. Bekefi and R. E. Shefer, "Stimulated Raman scattering by an intense relativistic electron beam subjected to a ripple electric field," *J. Appl. Phys.*, vol. 50, no. 8, pp. 5158-5164, 1979.
[9] V. L. Granatstein and P. Sprangle, "Mechanisms for coherent scattering of electromagnetic waves from relativistic electron beams," *IEEE Trans. Microwave Theory Tech.*, vol. MIT-25, p. 545, June 1977.
[10] J. Fajans, G. Bekefi, Y. Z. Yin, and B. Lax, "Microwave studies of a tunable free-electron laser in combined axial and wiggler guide fields," *Phys. Fluids*, vol. 28, no. 6, pp. 1995-2006, 1985.
[11] W. A. McMullin and G. Bekefi, "Stimulated emission from relativistic electrons passing through a spatially periodic longitudinal magnetic field," *Phys. Rev.*, vol. A25, no. 4, pp. 1826-1837, 1982.
[12] A. A. Grossman, T. C. Marshall, and S. P. Schlesinger, "A new millimeter free electron laser using a relativistic electron beam with spiraling electrons," *Phys. Fluids*, vol. 26, no. 1, pp. 337-343, 1983.
[13] P. C. Efthimion and S. P. Schlesinger, "Stimulated Raman scattering by an intense relativistic electron beam in a long ripple magnetic field," *Phys. Rev.*, vol. A16, no. 2, pp. 633-639, 1977.
[14] R. M. Gilgenbach, T. C. Marshall, and S. P. Schlesinger, "Spectral properties of stimulated Raman radiation from an intense relativistic electron beam," *Phys. Fluids*, vol. 22, no. 5, pp. 971-977, 1979.
[15] G. G. Denisov *et al.*, "Powerful electromagnetic millimeter wave oscillations produced by stimulated scattering of microwave radiation by electron beams," *Int. J. Infrared Millimeter Waves*, vol. 5, no. 10, pp. 1389-1403, 1984.
[16] Y. Carmel, V. Granatstein, and A. Gover, "Demonstration of a two-stage backward wave oscillator free-electron laser," *Phys. Rev. Lett.*, vol. 51, no. 7, pp. 566-569, 1983.
[17] R. A. Kehs *et al.*, "A high-power backward wave oscillator driven by a relativistic electron beam," *IEEE Trans. Plasma Sci.*, vol. PS-13, pp. 559-562, Dec. 1985.
[18] Yu. V. Tkach *et al.*, "Emission by a relativistic beam at a magneto-Cerenkov resonance in a periodic waveguide," *Sov. J. Plasma Phys.*, vol. 5, no. 5, pp. 566-570, 1979.
[19] R. A. Kehs, Y. Carmel, V. L. Granatstein, and W. W. Destler, "Experimental demonstration of an electromagnetically pumped free-electron laser with a cyclotron harmonic idler," *Phys. Rev. Lett.*, vol. 60, no. 4, pp. 279-281, 1988.
[20] R. A. Kehs, Y. Carmel, V. L. Granatstein, and W. W. Destler, "Experimental results from an electromagnetically pumped free electron laser with cyclotron harmonic idlers," in *Proc. BEAMS 88—7th Int. Conf. High-Power Particle Beams* (Karlsruhe, FRG), 1988, pp. 1281-1286.
[21] T. C. Marshall, *Free Electron Lasers*. New York: Macmillan, 1985.
[22] C. Roberson and P. Sprangle, "A review of free-electron lasers," *Phys. Fluids*, vol. B1(a), pp. 3-42, 1989.
[23] V. L. Bratman *et al.*, "Stimulated scattering of waves in microwave generators with high-current relativistic beams: Simulated of two-stage FEL," *Int. J. Electron.*, vol. 59, no. 3, pp. 247-289, 1985.
[24] H. P. Freund, "Efficiency enhancement in free electron lasers driven by electromagnetic-wave wigglers," *IEEE J. Quantum Electron.*, vol. QE-23, pp. 1590-1592, Sept. 1987, and references therein.

T. M. Tran. B. G. Danly, and J. S. Wurtele, "Free-electron lasers with electromagnetic standing wave wigglers," *IEEE J. Quantum Electron.*, vol. QE-23, pp. 1578–1589, Sept. 1987, and references therein.

[25] R. E. Collin, *Foundations for Microwave Engineering*. New York: McGraw-Hill, 1966, chap. 9.
C. C. Johnson, *Field and Wave Electrodynamics*. New York: McGraw-Hill, 1965, chap. 8.

[26] R. A. Kehs *et al.*, "DRAGON: A low impedance megavolt modulator for performing relativistic electron beam experiments," in *Proc. 16th Power Modulator Symp.* (Rosslyn, VA), 1984, pp. 203–206.

[27] C. B. Wharton, "High power microwave technology and diagnostics," in *High-Power Microwave Sources*, V. L. Granatstein and I. Alexeff, Eds. Boston, MA: Artech, 1987, chap. 2.

[28] J. Fisher, D. A. Boyd, A. Cavallo, and J. Benson, "Ten-channel grating polychromator for electron cyclotron emission plasma diagnostics," *Rev. Sci. Instrum.*, vol. 54, no. 9, pp. 1085–1090, 1983.

[29] A. Bromborsky and B. G. Ruth, "Calculation of the TM_{0n} dispersion relations in a corrugated cylindrical waveguide," *IEEE Trans. Microwave Theory Tech.*, vol. MTT-32, pp. 600–605, June 1984.

[30] J. A. Swegle, "Starting conditions for relativistic backward wave oscillators at low currents," *Phys. Fluids*, vol. 30, no. 4, pp. 1201–1211, 1987.

[31] V. L. Bratman *et al.*, "Relativistic gyrotrons and cyclotron autoresonant masers," *Int. J. Electron.*, vol. 51, no. 4, pp. 541–567, 1981.

[32] J. L. Vomvorides, "An efficient Doppler-shifted electron cyclotron maser oscillator," *Int. J. Electron.*, vol. 53, no. 6, pp. 555–571, 1982.

[33] V. L. Bratman, G. G. Denisov, N. S. Ginzburg, and M. I. Petelin, "FEL's with Bragg reflection resonators: Cyclotron autoresonance masers versus ubitrons," *IEEE J. Quantum Electron.*, vol. QE-19, pp. 282–296, Mar. 1983.

[34] P. Sprangle and R. A. Smith, "Theory of free-electron lasers," *Phys. Rev.*, vol. A21, no. 1, pp. 293–301, 1980.

[35] L. R. Elias, "High-power, CW efficient, tunable (UV through IR) free-electron laser using low-energy electron beams," *Phys. Rev. Lett.*, vol. 42, no. 15, pp. 977–981, 1980.

*

R. Alan Kehs (S'68–M'75–SM'88) received the B.S. and M.S. degrees in electrical engineering, and the M.S. and Ph.D. degrees in physics from the University of Maryland, College Park, in 1970, 1973, 1984, and 1987, respectively.

He has been employed by the Harry Diamond Laboratories, Adelphi, MD, since 1975, where his research interests have centered on the generation and use of intense relativistic electron beams—with emphasis on the production of high-power microwave radiation.

Dr. Kehs is a member of Eta Kappa Nu, Sigma Xi, and the American Physical Society.

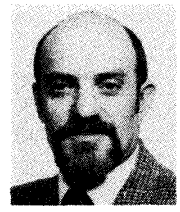

Yuval Carmel (S'66–M'74) was born in Israel in 1942. He received the B.Sc.(EE) and M.Sc.(EE) degrees from the Technion, Israel Institute of Technology, in 1966 and 1971, respectively, and the Ph.D.(EE) degree from Cornell University, Ithaca, NY, in 1974.

He was with the Government of Israel, the Naval Research Laboratory, and is currently with the University of Maryland, College Park. His research interests include electromagnetic radiation from intense electron beams, free electron lasers, advanced concepts in millimeter-wave tubes, gyrotrons, and backward wave oscillators.

*

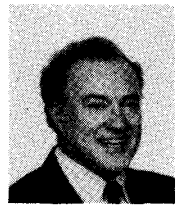

Victor L. Granatstein (S'59–M'64–SM'86) received the Ph.D. degree in 1963 from Columbia University, New York City, in electrical engineering and plasma physics.

After a year of postdoctoral work at Columbia University, he was a member of the Technical Staff of Bell Telephone Laboratories from 1964–1972. During 1969–1970 he was a Visiting Senior Lecturer at the Hebrew University of Jerusalem. In 1972 he joined the Naval Research Laboratory as a Research Physicist and from 1978–1983 served as Head of the High-Power Electromagnetic Radiation Branch. In August 1983 he became a Professor in the Electrical Engineering Department at the University of Maryland, College Park, and also serves as a Consultant to the Naval Research Laboratory, the Science Applications International Corporation, the Jet Propulsion Laboratory, and the State of Maryland (Department of Natural Resources). He is presently leading experimental and theoretical studies of electromagnetic radiation from relativistic electron beams, advanced concepts in millimeter-wave tubes, free electron lasers, and gyrotron amplifiers. He is Associate Editor of the *International Journal of Electronics* and has been a Guest Editor of the IEEE TRANSACTIONS ON MICROWAVE THEORY AND TECHNIQUES and the IEEE JOURNAL OF QUANTUM ELECTRONICS. He has been a reviewer for the NSF, AFOSR, DOE DNA, ONR, and ARO. He has co-authored more than 100 research papers in regular journals, and holds a number of patents on active and passive microwave devices. Since 1988 he has been Director of the Laboratory for Plasma Research at the University of Maryland.

Professor Granatstein is a Fellow of the American Physical Society.

*

William W. Destler (M'84), photograph and biography not available at the time of publication.